# Foxc2 in pharyngeal arch mesenchyme is important for aortic arch artery remodelling and ventricular septum formation

# Foxc2 in pharyngeal arch mesenchyme is important for aortic arch artery remodelling and ventricular septum formation

Mohammad Khaja Mafij Uddin[1], Wataru Kimura[2],Tomoyuki Ishikura[3],Haruhiko Koseki[3],Nobuaki Yoshida[4], Mohammod Johirul Islam[1], Mohammed Badrul Amin[1], Kasumi Nakamura[1], Yi-Xin Wu[1], Eiji Sato[1], Kazushi Aoto[1]*, Naoyuki Miura[1]

[1]Department of Biochemistry, Hamamatsu University School of Medicine, 1-20-1 Handayama Hamamatsu 431-3192, Japan

[2]Division of Cardiology, Department of Internal Medicine, UT Southwestern Medical Center, 6000 Harry Hines Blvd. Dallas, Texas 75390, U.S.A.

[3]Laboratory for Developmental Genetics, RIKEN Center for Integrative Medical Sciences (IMS-RCAI)

[4]Laboratory of Developmental Genetics, Center for Experimental Medicine and Systems Biology, Instituteof Medical Science, University of Tokyo, 4-6-1 Shirokanedai, Minato-ku, Tokyo 108-8639, Japan.

*Correspondence to: Department of Biochemistry, Hamamatsu University School of Medicine, 1-20-1 Handayama Hamamatsu 431-3192, Japan. Fax: +81-534352327. Phone: +81-534352327. Email address: kaz@hama-med.ac.jp

Running title: Foxc2 is required for aortic arch remodelling

**ABSTRACT**

The forkhead box c2 (Foxc2) protein is a member of the forkhead/winged helix transcription factor family and plays an essential role in cardiovascular development. Previous studies showed that *Foxc2* null mouse embryos die during midgestation or just after birth with severe cardiovascular defects, including interruption, coarctation of the aortic arch and ventricular septal defects. These are also seen in human congenital heart disease. However, the tissue specific role of Foxc2 in aortic arch remodelling is not yet fully understood. Here we show that Foxc2 is expressed in a restricted pattern in several cell populations, including the mesenchyme and endothelium of pharyngeal arch arteries, which are important for cardiovascular development. In this study, we use a conditional knockout approach to examine the tissue specific role of Foxc2 in aortic arch remodelling. We demonstrate that mouse embryos lacking Foxc2 in *Nkx2.5*-expressing mesenchyme and endothelium of pharyngeal arch arteries display aortic arch interruption type B and ventricular septal defects. In contrast, conditional deletion of *Foxc2* in *Tie2*-expressing endothelial cells does not result in aortic arch or ventricular septal defects, but does result in embryonic lethality due to peripheral oedema. Our data therefore provide for a detailed understanding of the role of mesenchymal Foxc2 in aortic arch remodelling and in the development of ventricular septum.

Human congenital heart defects are the most common birth defect, affecting 9 in 1000 live births (28). Outflow tract defects, aortic arch malformation and ventricular septal defects (VSD) are common forms of human congenital heart disease (14). In vertebrates, the heart is the first organ that develops through a complicated series of morphogenetic events involving the interaction between cells of different embryonic sources (3, 23). The mature aortic arch and great vessels derive from the embryonic pharyngeal arch arteries and the aortic sac. Five pairs of pharyngeal arch arteries appear in a rostrocaudal direction during embryogenesis and form the precursors of the great vessels and large arteries in the head and neck. Arch arteries develop from the aortic sac and end in the dorsal aorta and finally contribute to specific arteries (25). At embryonic day 9.5 (E9.5) in mice the first and second arch arteries appear. At E10.5, the first and second arch arteries disappear, while the third, fourth and sixth arch arteries are appeared. All arch arteries undergo a remodelling process to correctly establish an embryonic and postnatal circulatory system. Asymmetrically programmed regression and persistence of specific arch arteries are involved in the remodelling process. Until E15.5, the aortic arch is formed by remodelling of the aortic sac, the left fourth arch artery and left dorsal aorta. The right fourth arch artery contributes to the brachiocephalic artery and proximal part of the right subclavian artery. The left sixth arch artery remodels into the pulmonary trunk and ductusarteriosus Botalli, while the right sixth artery regresses and ultimately disappears. The right and left third arch artery reform into the bilateral common carotid arteries (6-8,25).

Forkhead box C2 (Foxc2)/mesenchymal forkhead-1 is a member of the forkhead family of transcription factors. Foxc2 is strongly expressed in the developing heart, limb, lymphatic and blood vessels, cartilaginous tissues, head mesenchyme, kidney, bones and dorsal aortas, suggesting that it is involved in a wide variety of developmental processes (19). Foxc2 plays an

essential role in the vascular/lymphatic vessel formation in cardiovascular development and diseases. Mutations in *FOXC2* in humans cause lymphedema-diatichiasis syndrome (LD syndrome), a rare autosomal dominant genetic multisystem disorder characterised by swelling of the legs because of fluid accumulation, and the development of extra eyelashes (distichiasis). Congenital heart disease occurs in 7% of individuals with LD syndrome. Additional anomalies sometimes associated with this disorder include ventricular and atrial septal defects, patent ductusarteriosus, cleft palate, and abnormal heart rhythm (16). Foxc2 is important for the remodelling of pharyngeal arch arteries to the aortic arch. Our laboratory and others have shown that null mutation of *Foxc2* causes perinatal lethality, a defective lymphatic system, skeletal malformation and aortic arch patterning defects (6). The most common aortic arch patterning defect is an interrupted aortic arch type B (IAA-B), in which part of aortic arch between the left common carotid artery and left subclavian artery is interrupted (6, 30).

It has been previously shown that Foxc2 mRNA is expressed in the pharyngeal arch artery mesenchyme and endothelial cells (6). To investigate the tissue-specific requirement of Foxc2 signalling in remodelling of the aortic arch, we generated *Foxc2* conditional knockout mice. We generated mice with *Foxc2* specifically knocked out either in the mesenchyme and the endothelium, or only in the endothelium. We found that all *Foxc2* conditional mutant embryos die just after birth due to cardiac abnormalities. Furthermore, *Foxc2* ablation in the mesenchyme by *Nkx2.5-Cre* mice causes an interrupted aortic arch and other cardiovascular defects.

## MATERIALS AND METHODS

*Generation of Foxc2 conditional knockout mice.* A genomic DNA fragment containing the coding exon of the mouse *Foxc2* gene (18) was isolated from a 129/SvJ mouse genomic library (Stratagene, CA, USA). A loxP DNA fragment was inserted into the 5' untranslated region (UTR) of this *Foxc2* gene. Another loxP DNA and FRT-flanked neomycin resistant gene ($Neo^R$) under control of the PGK promoter was inserted into the 3' UTR to enable positive selection (31). Diphtheria toxin A (DTA) gene and thymidine kinase (TK) gene under control of the polyoma enhancer/herpes simplex virus thymidine kinase (MC1) promoter were inserted flanking the 5' and 3' UTRs respectively (Fig. 1A). DTA was used as a negatively selective marker that allows for selection against unwanted random integrants. The $Neo^R$ cassette was used for positive selection of cells containing an integrated copy of the targeting vector using G418 (Sigma Aldrich, Co., USA), whereas TK was used as a negatively selective marker for randomly integrated cells using gancyclovir (17, 32).

The targeting vector was electroporated into embryonic stem cells (ES) and G418 and gancyclovir resistant ES colonies were picked and subjected to Southern blot analysis using *Hind*III & *Sac* I cut labeled probe (Fig.1B, black bar). Two clones were obtained and were used to generate chimeric mice as described previously (27). Chimeric mice were crossed with female C57BL/6J mice to obtain *Foxc2* $^{floxed\ (fl)\text{-}neo}$ mice. These mice were then crossed with *Act-FLPe* mice (24) to remove the FRT-flanked PGK-$Neo^R$ cassette, thus generating *Foxc2* $^{fl/+}$ mice (Fig. 1A). The genotype of adult mice or embryos was determined by polymerase chain reaction (PCR) analysis using 3 primers, A: 5'-ACTCGCACCGGCTAGGACTG-3',B:5'GCATCTGGGTAGGGGAACG-3', C: 5'-ATCACTTGAACTCCGCGCCCTG-3'. The

wild-type and *Foxc2* $^{fl}$ alleles generate amplicons of 360 bp and 600 bp respectively (Fig. 1C). *Foxc2* $^{fl/+}$ heterozygote mice were intercrossed to make homozygote. Homozygote *Foxc2*$^{fl/fl}$ mice were fertile and did not show any phenotypical and histological abnormalities.

*Mouse strain maintenance.* *Nkx2.5-Cre* knock-in mice, *Tie2-Cre* transgenic mice and *R26R* reporter mice were described previously (11, 21, 26). All mice were maintained by continual crossing with C57BL/6J mice. *Foxc2*$^{fl/fl}$ mice were maintained as homozygotes in their own strain background. Mesenchymal and endothelial cell-specific *Foxc2* conditional knockout (cKO) mice were obtained as follows. In the first cross, *Nkx2.5-Cre* or *Tie2-Cre* male mice were mated with female *Foxc2*$^{fl/fl}$ mice to generate *Nkx2.5-Cre;Foxc2*$^{fl/+}$ and *Tie2-Cre;Foxc2*$^{fl/+}$ male mice respectively. These male mice were subsequently crossed with *Foxc2*$^{fl/fl}$ mice to obtain *Nkx2.5-Cre; Foxc2*$^{fl/fl}$ and *Tie2-Cre; Foxc2*$^{fl/fl}$ conditional knockout embryos for analysis. Genotyping of mice and embryos was carried out by allele-specific PCR. The animal experimental procedures conducted in this study were reviewed and approved by the Hamamatsu University School of Medicine Committee on Laboratory Animals.

*Intracardiac ink injection.* For examination of aortic arch remodelling, embryos between E12.5 and E13.5 were selected. Indian ink (Winsor & Newton Ink, England) was injected into the left ventricle of the heart using custom-made glass pipettes. After injection embryos were fixed overnight in 4% paraformaldehyde (PFA, Sigma-Aldrich, Co., USA) at 4°C, dehydrated through a series of methanol/phosphate buffer saline (PBS) to 100% methanol and cleared in 2:1 ratio of benzyl benzoate and benzyl alcohol (NacalaiTesque, Inc., Japan). Images were acquired with a Leica MZ6 microscope using an Olympus DP12 digital microscope camera.

*X-gal staining.* For whole-mount X-gal staining, dissected embryos were isolated in ice-cold PBS and fixed with 0.2% glutaraldehyde (Wako Pure Chemical Industries, Ltd.) at 4°C for 10 min, washed in PBS and stained for X-gal (5- bromo-4-chlro-3-indoyl β-D-galactopyranoside, Takara Biochemicals, Japan) solution at 37°C overnight. For X-gal staining on sections, dissected embryos were fixed in 4% PFA/ PBS on ice for 30 min and then processed through graded sucrose/PBS solutions (5%, 10%, 15% and 20%) until the embryos sank. The embryos were embedded in Tissue-Tek O.C.T. compound (Sakura Finetek Japan) and stored at -85°C.Sections, 10 μm thickness were obtained using a cryostat and rinsed with buffer containing 2 mM magnesium chloride, 0.02% NP-40, and 0.01% sodium deoxycholate. The sections were then stained in the same buffer with 5mM potassium ferricyanide, 5 mM potassium ferrocyanide and 1mg/mL X-gal at 37°C. The stained slides were then washed, postfixed in 4% PFA/PBS, dehydrated in an ethanol/xylene series and mounted in Mount-Quick mounting medium (Daido Sangyo Co., Japan). Whole mount and section X-gal staining was carried out on five heterozygous mice. Images were captured with an Olympus DP72 digital camera through an Olympus BX-51 microscope.

*Histology.* Dissected embryos were fixed in 4% PFA/PBS, dehydrated in an ethanol/xylene series and embedded in paraffin wax by standard procedures. Sections, 10 μm thickness were dewaxed, rehydrated in a xylene/ethanol series, and stained with haematoxylin/eosin solution (H&E) by standard procedures. Sectional images were acquired using an Olympus BX-51 light microscope and an Olympus DP72 digital camera. H&E staining was carried out on a minimum of five control and five mutant embryos.

*Immunofluorescence microscopy.* Immunofluorescence staining was performed as previously described (2). Dissected embryos were fixed in 1% formalin/PBS (Wako Pure Chemical Industries, Ltd.) overnight at 4°C. Embryos were processed in graded sucrose and embedded in O.C.T. compound. Frozen sections (10 μm) were incubated in a blocking buffer (3% bovine serum albumin, 0.1% Tween-20 in PBS) for 1h. Sections were incubated with rat monoclonal anti-mouse Foxc2 antibody (4) diluted 1:1,000 in blocking solution overnight at 4°C. Sections were washed and then incubated with Alexa fluor488 donkey anti-rat IgG (1:200, Life technologies) for 1 h at room temperature. All slides were stained with the nuclear marker DAPI (DOJINDO Molecular Technologies, Inc). Images were taken using a confocal laser scanning microscope (FluoView FV1000, Olympus).

## RESULTS

### *Generation of conditional Foxc2$^{fl/fl}$* mice

To investigate the tissue specific role of Foxc2 during embryonic development, a targeting vector containing *Foxc2* conditional allele was electroporated into the mouse ES cells and the ES colonies were selected with G418 and gancyclovior (Fig. 1A). Two clones containing the *Foxc2 $^{floxed\text{-}neo}$*-targeted alleles were identified from 500 screened clones. Correct targeting vector of homologous regions was confirmed by Southern blot analysis. For Southern blot analysis, genomic DNA was isolated from ES cells and digested with *Xba*I, transferred to nylon membrane and then hybridized with *Hind* III & *Sac* I cut probe. The *Foxc2$^{fl\text{-}neo}$* allele was detected as 5.6 kbp whereas Foxc2 allele was detected as 12.7 kbp (Fig. 1B). Targeted ES cells for *Foxc2$^{fl\text{-}neo}$* were used to produce chimeric mice by blastocyst injection. Male chimeras were mated with C57BL/6J females to obtain *Foxc2$^{fl\text{-}neo}$* mice. *Foxc2$^{fl\text{-}neo}$* mice were further crossed with *Act-FLPe* mice to remove the Neo$^{R}$ cassette and the TK genes in the germ line to make *Foxc2$^{fl/+}$* mice. These mice were intercrossed to produce homozygotes and this was confirmed by PCR (Fig. 1C).

### *Nkx2.5-Cre and Tie2-Cre expression in the pharyngeal arches*

Previous studies showed that *Nkx2.5-Cre* expression was first detected as early as E7.5 in the cardiac crescent and pharyngeal endoderm and *Tie2-Cre* expression was detected in all endothelial cells at E9.5 (11, 21). To investigate *Nkx2.5-* and *Tie2*-directed expression of *Cre* recombinase, we crossed our Cre mice with the *R26R* reporter mice, which express β-galactosidase (β-gal) only in the presence of *Cre* recombinase. *Nkx2.5-Cre; R26R* and *Tie2-Cre; R26R* embryos at E10.5 were stained for X-gal to reveal *Cre* mediated β-gal activity. Usually, the

heart field is patterned into primary heart field and secondary heart field on the basis of molecular, genetic and morphological events. The primary heart field contributes mostly to the left ventricle and the left and right atrium, whereas the secondary heart field develops mainly into the right ventricle, outflow tract and both atria (1, 34). In *Nkx2.5-Cre; R26R* embryos, strong β-gal activity was detected in the pharyngeal arch core mesoderm and secondary heart field (Fig. 2A). Frontal sections of *Nkx2.5-Cre; R26R* compound heterozygote mice showed that *Nkx2.5*-driven *Cre* activity is strongly expressed in the mesenchyme surrounding the third, fourth and sixth pharyngeal arch arteries. β-gal activity was also detected in endothelium, endoderm and ectoderm of pharyngeal arches (Fig. 2B-C). These results are consistent with previously published data (21). *Tie2-Cre* transgene is driven by an endothelium-specific receptor, tyrosine kinase promoter/enhancer. *Tie2* expression persists in the endothelial cells throughout embryogenesis. Whole-mount X-gal staining in *Tie2-Cre; R26R* mice showed that β-gal is uniformly detectable in the endothelial cells lining the lumen of all blood vessels (Fig. 2D). Frontal sections of E10.5 embryos showed that β-gal is strongly expressed in the endothelium of the pharyngeal arches whereas mesenchymal cells were completely negative for β-gal staining (Fig. 2E-F). *Tie2-Cre* expression was also consistent with the previous study (11). These results revealed that *Nkx2.5-Cre* was expressed in both endothelium and mesenchyme of pharyngeal arch arteries whereas *Tie2-Cre* was expressed only in the endothelium, as expected.

*Mesenchymal and endothelial specific Foxc2 deletion*

To investigate the cell type-specific expression of Foxc2, immunostaining in the developing pharyngeal arch arteries was carried out. In E10.5control ($Foxc2^{fl/fl}$) embryos, Foxc2 protein was strongly expressed in the endothelial cells and surrounding mesenchymal cells of third, fourth and sixth pharyngeal arch arteries (Fig. 3A-C). This protein expression data is consistent with

our previous observation of *Foxc2* mRNA expression in the arch arteries (6). These data suggest that Foxc2 is expressed in the same regions as *Nkx2.5* and *Tie2*, i.e. that of mesenchyme and endothelium of pharyngeal arches (Fig. 2).

To determine whether Foxc2 expression in *Nkx2.5*-expressing mesenchymal and endothelial cells is required for correct development of the pharyngeal arches, we performed conditional deletion of *Foxc2* by crossing our $Foxc2^{fl/fl}$ mice with *Nkx2.5-Cre* and *Tie2-Cre* mice. Immunostaining with anti-Foxc2 antibody and confocal microscopy of *Nkx2.5-Cre;* $Foxc2^{fl/fl}$ embryonic sections at E10.5 revealed that *Foxc2* was efficiently deleted in the mesenchymal cells surrounding the endothelium of the pharyngeal arches compared to control embryos (Fig. 3D-F). To determine whether expression of Foxc2 in the endothelium of the pharyngeal arches is required for aortic arch remodelling, *Foxc2* was conditionally deleted in the endothelium by crossing our $Foxc2^{fl/fl}$ mice with *Tie2-Cre* mice. Immunostaining and confocal microscopy of E10.5 *Tie2-Cre;* $Foxc2^{fl/fl}$ embryonic sections revealed that *Foxc2* was efficiently deleted specifically in the endothelial cells, whereas the mesenchymal expression of the pharyngeal arch arteries was unaffected (Fig. 3G-I). These data clearly indicate that *Nkx2.5-Cre* efficiently inactivated *Foxc2* both in the mesenchyme and in the endothelium of the pharyngeal arch arteries whereas *Tie2-Cre* deleted *Foxc2* only in the endothelium of the pharyngeal arches.

*Mesenchymal Foxc2 inactivation causes interrupted aortic arch*

Previous studies have shown that *Foxc2* null mice died prenatally or perinatally with cardiovascular defects, suggesting that the severity of the defect may be caused by different cell type-specific Foxc2 functions (6, 30). In most cases, abnormalities are associated with aortic arch interruption, coarctation or hypoplasia of the fourth arch arteries and VSD (6, 30). E18.5 control

(*Foxc2* $^{fl/fl}$), *Nkx2.5-Cre; Foxc2*$^{fl/fl}$ and *Tie2-Cre; Foxc2*$^{fl/fl}$ mutant embryos were examined for cardiac abnormalities. Upon careful gross anatomical examination, we found that in control embryos, the left common carotid, left subclavian and right brachiocephalic arteries branch directly from the ascending aorta. This indicates normal aortic arch formation in control embryos (Fig. 4A). We observed that all of *Nkx2.5-Cre; Foxc2*$^{fl/fl}$ conditional mutant embryos (n=7) showed an aortic arch remodelling defect (Table 1). This defect included an interrupted aortic arch type B (IAA-B), where part of the aortic arch between the left common carotid artery and the left subclavian artery was missing (Fig. 4B). We did not find any *Tie2-Cre; Foxc2*$^{fl/fl}$ embryos with aortic arch interruption (Fig. 4C), suggesting that Foxc2 in the mesenchyme plays an important role in aortic arch remodelling.

*Nkx2.5-Cre- and Tie2-Cre-specific deletion of Foxc2 results in other cardiovascular defects*

Next we examined whether any other cardiovascular defect is present in the conditional mutant embryos. A summary of the cardiovascular and other defects is shown in Table 1. Histological examination of E18.5 control heart showed that ventricles are well separated (Fig. 5A). Transverse sections of E18.5 *Nkx2.5-Cre; Foxc2*$^{fl/fl}$ embryos showed VSD where membranous portions of the ventricular septum failed to fuse (Fig. 5B). In contrast, we did not find any VSD in the *Tie2-Cre* endothelial-specific conditional *Foxc2* mutant embryos, which were very similar to control embryos (Fig. 5C). These results were consistent with our observation where we did not find any aortic arch interruption in the *Tie2-Cre; Foxc2*$^{fl/fll}$ conditional mutant embryos at E18.5. These data suggest that aortic arch interruption has some correlation with VSD. With microscopic examination of E14.5 control and mutant embryos, we did not find any gross structural abnormalities in the control (Fig. 5D) and *Nkx2.5-Cre; Foxc2*$^{fl/fl}$ conditional mutant embryos (Fig. 5E). These embryos displayed spontaneous movements and cardiac pulsations. On

the other hand, *Tie2-Cre; Foxc2*$^{fl/fl}$ embryos showed peripheral oedema that may be due to the accumulation of pericardial effusion (Fig. 5F). In these mice, embryonic lethality was likely to be secondary to the heart failure.

*Mesenchymal Foxc2 is required for aortic arch remodelling in the critical stage*

Our data clearly indicate that *Foxc2* conditional mutant embryos showed cardiovascular phenotypes such as interrupted aortic arch and VSD. To explore the critical stage of Foxc2 function in aortic arch remodelling, we performed India ink injection at E12.5 and E13.5 in control and mutant embryos. At E12.5, aortic arch remodelling was comparable between control (Fig. 6A) and *Nkx2.5-Cre; Foxc2*$^{fl/fl}$ conditional mutant embryos (Fig. 6B). Aortic arch remodelling defect was clearly apparent at E13.5 in *Nkx2.5-Cre; Foxc2*$^{fl/fl}$ embryos (Fig.6D) as compared to control embryos (Fig. 6C). In *Tie2-Cre; Foxc2*$^{fl/fl}$ embryos, aortic arch patterning was normal, i.e. similar to controls (data not shown). These results indicate that *Foxc2* inactivation in the mesenchyme does not affect the initial formation and patterning of pharyngeal arch arteries, but causes their defective remodelling at a later stage.

## DISCUSSION

In this study, we present convincing evidence demonstrating that inactivation of *Foxc2* from the *Nkx2.5*-expressing cells leads to cardiovascular defects including interrupted aortic arch type B and VSD.

Pharyngeal arch arteries are initially formed as bilateral symmetric vessels. During aortic arch remodelling, some of the arch artery segments degenerate while other segment remain and contribute to definitive left sided aortic arch and major vessels in the adult. This remodelling is a complex process governed by a signalling network that remains poorly understood. Previously, the functions of Foxc2 for normal development of the aortic arch have been analysed. Simple knockout of Foxc2 in mice showed aortic arch remodelling defect, skeletal malformation and other cardiovascular defects. Foxc2 is required for extensive remodelling of the dorsal aorta and arch arteries, particularly the fourth arch artery, to form the aortic arch (6).

In this study, we examined the expression of Foxc2 in the pharyngeal arch arteries of E10.5 control and mutant mouse embryos by immunostaining. Foxc2 was strongly expressed in the surrounding mesenchymal cells and endothelium of the third, fourth and sixth pharyngeal arch arteries of control embryos (Fig. 3 A-C). Information regarding Foxc2 expression in cardiac progenitors during critical stages of aortic arch remodelling has been poorly described and it is not clear in which cell populations Foxc2 plays a role in aortic arch remodelling. We therefore considered the *Cre*-driver strategy to be an effective way to cell type-specific deletion of Foxc2 in aortic arch remodelling. We ablated *Foxc2* using mesenchyme- and endothelial-specific *Cre* mice. X-gal staining confirmed *Nkx2.5* expression in mesenchyme and endothelium and *Tie2* expression in endothelial cells of the pharyngeal arch arteries (Fig. 2). Mesenchyme specific

deletion of *Foxc2* in *Nkx2.5-Cre; Foxc2$^{fl/fl}$* mice showed interrupted aortic arch type B. This phenotype is also common in DiGeorge syndrome in humans which is characterized by microdeletion of chromosome 22q11.2 (29). This result provides the first evidence of a tissue-specific role of Foxc2 in aortic arch remodelling. Type B interruption of the aortic arch was also found in *endothelin-1* deficient mice (12). This is also observed in mice in which *Bmp4* is conditionally inactivated within the *Tbx1* expression domain (22), and it is of note that in these mice the initial patterning is normal, a feature that is very similar to our mutant mice. *Bmp4* knockout study showed *Bmp4* requirement for recruitment/differentiation of smooth muscle cells surrounding the pharyngeal arch arteries (22). Section *in situ* hybridization method for *Bmp4* mRNA showed reduced expression in *Nkx2.5-Cre; Foxc2$^{fl/fl}$* mutant embryos compared to control (data not shown). This data suggest that *Foxc2* has association with *Bmp4* signalling in the mesenchyme of pharyngeal arch arteries. Our histologic analysis showed VSD only in *Nkx2.5-Cre; Foxc2$^{fl/fl}$* mutant embryos. Inactivation of *Foxc2* may cause the loss of *Bmp4* function for growth of the contruncal mesenchyme necessary for septum formation (22). Loss of function of several other genes including pitx2c, Crkl, Tgfβ causes interrupted aortic arch in addition to other cardiovascular defects (5, 15, 20). We also found IAA-B when *Foxc2* was inactivated using secondary heart field specific *Isl1-Cre* and *Tbx1-Cre* mice (unpublished data). Recent studies showed that *Nkx2.5* is expressed in the first heart field, second heart field pharyngeal mesoderm and its adjacent endodermal cells (34). Interestingly, our *Nkx2.5-Cre; Foxc2$^{fl/fl}$* mutant embryos showed IAA-B; these data support the fact that *Nkx2.5* is expressed in some part of the secondary heart field in addition to the primary heart field. In contrast to *Nkx2.5-Cre; Foxc2$^{fl/fl}$* mutant, no aortic arch defect was observed in *Tie2-Cre; Foxc2$^{fl/fl}$* mutant embryos. Severe peripheral oedema was observed in *Tie2-Cre; Foxc2$^{fl/fl}$* mutant embryos, which was considered

to result in embryonic lethality. These results suggest that Foxc2 is also involved in the embryonic lymphatic vessels development that are associated with LD syndrome.

Previous studies showed that half of the *Foxc2* null embryos died during gestation and those remaining died just after birth, whereas, *Foxc2* conditional embryos only died just after birth (Table1). The neonatal embryonic death may be due to the inability to inhale air into the lungs in addition to interruption of the aortic arch. Our results showed normal aortic arch patterning when intracardiac ink injection was performed into the heart of E12.5 control and mutant embryos. At E13.5, the most common defect, seen in all *Nkx2.5-Cre; Foxc2*$^{fl/fl}$ mutant embryos, was absence of fourth arch artery derivatives, which led to the interruption of the aortic arch (Fig. 6). Cardiac neural crest cells ablation in chick embryos causes cardiovascular phenotypes including aortic arch remodelling defect. These data demonstrated that cardiac neural crest-derived cells are important for aortic arch remodelling (9, 10). It is clear from this and other studies that Foxc2 is not involved in the initial formation or patterning of pharyngeal arch arteries but affects their remodelling process. The morphology and final rearrangement of these great vessels require reciprocal signalling between neural crest cells-derived mesenchyme surrounding the arch arteries (13) and endothelial cells (33). Our results suggest that future studies are required to determine whether Foxc2 interacts with some secreted molecules or other transcription factors in the mesenchyme derived from cardiac neural crest cells surrounding pharyngeal arch arteries during the remodelling process.

In conclusion, our study clearly demonstrated that expression of Foxc2 in the mesenchyme of pharyngeal arch arteries is important for aortic arch remodelling. In addition to this, our conditional *Foxc2* mouse can be used as a powerful tool to reveal the molecular mechanisms and genetic determinant that are involved in aortic arch remodelling.

Acknowledgement

We would like to thank to Dr. Philippe Soriano at Mount Sinai Hospital, New York, USA for *R26R* mice. This work was supported by Research-in-Aid grants from the Ministry of Education, Science, Sports, Culture and Technology of Japan and from Hamamatsu University School of Medicine. We are also grateful to the Uehara Memorial Research Foundation and Otsuka Toshimi Scholarship Foundation for their support.

REFERENCES


1. Abu-Issa R and Kirby ML (2007) Heart field: from mesoderm to heart tube. *Annu Rev Cell Dev Biol* **23**, 45-68.
2. Aoto K and Trainor PA (2015) Co-ordinated brain and craniofacial development depend upon Patched1/XIAP regulation of cell survival. *Hum Mol Genet* **24**, 698-713.
3. Fishman MC and Chien KR (1997) Fashioning the vertebrate heart: earliest embryonic decisions. *Development* **124**, 2099-2117.
4. Furumoto TA, Miura N, Akasaka T, Mizutani-Koseki Y, Sudo H, Fukuda K, Maekawa M, Yuasa S, Fu Y, Moriya H, Taniguchi M, Imai K, Dahl E, Balling R, Pavlova M, Gossler A and Koseki H (1999) Notochord-dependent expression of MFH1 and PAX1 cooperates to maintain the proliferation of sclerotome cells during the vertebral column development. *Dev Biol* **210**, 15-29.
5. Guris DL, Fantes J, Tara D, Druker BJ and Imamoto A (2001) Mice lacking the homologue of the human 22q11.2 gene CRKL phenocopy neurocristopathies of DiGeorge syndrome. *Nat Genet* **27**, 293-298.
6. Iida K, Koseki H, Kakinuma H, Kato N, Mizutani-Koseki Y, Ohuchi H, Yoshioka H, Noji S, Kawamura K, Kataoka Y, Ueno F, Taniguchi M, Yoshida N, Sugiyama T and Miura N (1997) Essential roles of the winged helix transcription factor MFH-1 in aortic arch patterning and skeletogenesis. *Development* **124**, 4627-4638.
7. Kanzaki-Kato N, Tamakoshi T, Fu Y, Chandra A, Itakura T, Uezato T, Tanaka T, Clouthier D, Sugiyama T, Yanagisawa M and Miura N (2005) Roles of forkhead transcription factor Foxc2 (MFH-1) and endothelin receptor A in cardiovascular morphogenesis. *Cardiovasc Res* **65**, 711-718.

8. Kaufman MH, editor. The atlas of mouse development. Academic Press, Inc., San Diego, CA; 1992.

9. Kirby ML and Waldo KL (1990) Role of neural crest in congenital heart disease. *Circulation* **82**, 332-340.

10. Kirby ML and Waldo KL (1995) Neural crest and cardiovascular patterning. *Circ Res* **77**, 211-215.

11. Kisanuki YY, Hammer RE, Miyazaki J, Williams SC, Richardson JA and Yanagisawa M (2001) Tie2-Cre transgenic mice: a new model for endothelial cell-lineage analysis in vivo. *Dev Biol* **230**, 230-242.

12. Kurihara Y, Kurihara H, Oda H, Maemura K, Nagai R, Ishikawa T and Yazaki Y(1995) Aortic arch malformations and ventricular septal defect in mice deficient in endothelin-1. *J Clin Invest* **96**, 293-300.

13. Le Lievre CS and Le Douarin NM (1975) Mesenchymal derivatives of the neural crest: analysis of chimaeric quail and chick embryos. *J Embryol Exp Morphol* **34**, 125-54.

14. Lindsay EA, Botta A, Jurecic V, Carattini-Rivera S, Cheah YC, Rosenblatt HM, Bradley A and Baldini A (1999) Congenital heart disease in mice deficient for the DiGeorge syndrome region. *Nature* **401**, 379-383.

15. Liu C, Liu W, Palie J, Lu MF, Brown NA and Martin JF (2002) Pitx2c patterns anterior myocardium and aortic arch vessels and is required for local cell movement into atrioventricular cushions. *Development* **129**, 5081-5091.

16. Mansour S, Brice GW, Jeffery S and Mortimer P (2005) Lymphedema-Distichiasis Syndrome. *Genes reviews* (last updated 2012)

17. Mansour SL, Thomas KR and Capecchi MR (1988) Disruption of the proto-oncogene int-2 in mouse embryo-derived stem cells: a general strategy for targeting mutations to non-selectable genes. *Nature* **336**, 348-352.

18. Miura N, Iida K, Kakinuma H, Yang XL and Sugiyama T (1997) Isolation of the mouse (MFH-1) and human (FKHL 14) mesenchyme fork head-1 genes reveals conservation of their gene and protein structures. *Genomics* **41**, 489-492.

19. Miura N, Wanaka A, Tohyama M and Tanaka K (1993) MFH-1, a new member of the fork head domain family, is expressed in developing mesenchyme. *FEBS Lett* **326**, 171-176.

20. Molin DG, DeRuiter MC, Wisse LJ, Azhar M, Doetschman T, Poelmann RE and Gittenberger-de Groot AC (2002) Altered apoptosis pattern during pharyngeal arch artery remodelling is associated with aortic arch malformations in Tgfbeta2 knock-out mice. *Cardiovasc Res* **56**, 312-322.

21. Moses KA, DeMayo F, Braun RM, Reecy JL and Schwartz RJ (2001) Embryonic expression of an Nkx2-5/Cre gene using ROSA26 reporter mice. *Genesis* **31**(4), 176-80.

22. Nie X, Brown CB, Wang Q and Jiao K (2011) Inactivation of Bmp4 from the Tbx1 expression domain causes abnormal pharyngeal arch artery and cardiac outflow tract remodeling. *Cells Tissues Organs* **193**, 393-403.

23. Olson EN and Srivastava D (1996) Molecular pathways controlling heart development. *Science* **272**, 671-676.

24. Rodriguez CI, Buchholz F, Galloway J, Sequerra R, Kasper J, Ayala R, Stewart FA and Dymecki MS (2000) High-efficiency deleter mice show that FLPe is an alternative to Cre-loxP. *Nat Genet* **25**, 139-140.

25. Rugh R (1990) The mouse. Its reproduction and development. Oxford University Press, Inc.,Oxford, UK.

26. Soriano P (1999) Generalized lacZ expression with the ROSA26 Cre reporter strain. *Nat Genet* **21**, 70-71.

27. Tanaka T, Akira S, Yoshida K, Umemoto M, Yoneda Y, Shirafuji N, Fujiwara H, Suematsu S and Yoshida N (1995) Targeted disruption of the NF-IL6 gene discloses its essential role in bacteria killing and tumor cytotoxicity by macrophages. *Cell* **80**, 353-361.

28. Van der Linde D, Konings EE, Slager MA, Witsenburg M, Helbing WA, Takkenberg JJ and Hesselink –Roos W (2011) Birth prevalence of congenital heart disease worldwide: a systematic review and meta-analysis. *J Am Coll Cardiol* **58**, 2241-2247.

29. Wilson DI, Burn J, Scambler P and Goodship J (1993) DiGeorge syndrome: part of CATCH 22. *J Med Genet* **30**, 852-856.

30. Winnier GE, Hargett L and Hogan BL (1997) The winged helix transcription factor MFH1 is required for proliferation and patterning of paraxial mesoderm in the mouse embryo. *Genes Dev* **11**, 926-940.

31. Yagi T, Ikawa Y, Yoshida K, Shigetani Y, Takeda N, Mabuchi I, Yamamoto T and Aizawa S (1990) Homologous recombination at c-fyn locus of mouse embryonic stem cells with use of diphtheria toxin A-fragment gene in negative selection. *Proc Natl Acad Sci USA* **87**, 9918-9922.

32. Yagi T, Nada S, Watanabe N, Tamemoto H, Kohmura N, Ikawa Y and Aizawa S ( 1993) A novel negative selection for homologous recombinants using diphtheria toxin A fragment gene. *Anal Biochem* **214**, 77-86.

33. Yanagisawa H, Hammer RE, Richardson JA, Williams SC, Clouthier DE and Yanagisawa M (1998) Role of Endothelin-1/Endothelin-A receptor-mediated signaling pathway in the aortic arch patterning in mice. *J Clin Invest* **102**, 22-33.

34. Zhang L, Nomura-Kitabayashi A, Sultana N, Cai W, Cai X, Moon AM and Cai CL (2014) Mesodermal Nkx2.5 is necessary and sufficient for early second heart field development. *Dev Biol* **390**, 68-79.

Table 1. Summary of phenotypes of newborn pups

| Mouse genotype | Disorders | | | | |
|---|---|---|---|---|---|
| | Lethality | Cardiovascular | Craniofacial | Skeletal | others |
| *Foxc2-/-* | 50% die around E13.5 & rest of them die just after birth | IAA-B, IAA-C, VSD, Lymphatic vessel | Cleft Palate | Short vertebral column<br>Hypoplasia of bones | No |
| *Nkx2.5-Cre; Foxc2$^{fl/fl}$* | 100% Die just after birth (n=12) | IAA-B (n=7)<br>VSD (n=5) | No | No | No |
| *Tie2-Cre; Foxc2$^{fl/fl}$* | 100% Die just after birth (n=9) | Lymphatic vessel | No | No | Edema, pleural effusion |

IAA-B, interrupted aortic arch type B; IAA-C, interrupted aortic arch type C; VSD, ventricular septal defects.

## Figure Legends

**Fig.1** Generation of the conditional *Foxc2*$^{fl/fl}$ allele in mice. (A) Schematic representation of the targeting strategy employed to generate a floxed allele of *Foxc2*. The structure of *Foxc2* gene, targeted allele, *Foxc2* $^{flox\text{-}neo}$ allele and *Foxc2*$^{fl}$ allele are shown. Open reading frame is shown as a shaded box. The probe used for Southern blot analysis is indicated by a black box. Dashed lines demarcate the homologous fragments used in the targeting vector. Abbreviations for the restriction enzyme sites: Xb, *Xba*I; N, *Not*I. Solid arrowhead and open arrowhead indicate loxP and FRT-Neo$^{R}$ cassette, respectively. (B) Representative Southern blot analysis of DNA samples from non-recombinant and recombinant alleles. The 12.7 kbp wild-type (wt) and 5.6 kbp targeted mutant allele were identified by the designated probe. (C) PCR genotyping of DNA samples from the yolk sac of intercrossing between two *Foxc2*$^{fl/+}$ mice. The PCR products of 360 bp and 600 bp were identified as wild-type and *Foxc2*$^{fl/fl}$ alleles, respectively.

**Fig. 2** Expression pattern of *Nkx2.5-Cre* and *Tie2-Cre* using *R26R* reporter mice. (A) Whole-mount X-gal staining of *Nkx2.5-Cre; R26R* compound heterozygote mice at E10.5 embryos. β-gal activity was strongly detected in the pharyngeal arches and throughout the heart (white arrow). (B) Frontal sections of E10.5 embryos showed that *Nkx2.5-Cre* activity is strongly expressed in the mesenchymal cells (arrow) surrounding endothelial cells (arrowhead) of the pharyngeal arch arteries III, IV and VI. (C) High-power magnification of fourth pharyngeal arch artery showed strong *Nkx2.5-Cre* expression in the mesenchyme (arrow) and endothelium (arrowhead). (D) Whole-mount X-gal staining of E10.5 *Tie2-Cre; R26R* embryos showed uniform β-gal expression in the blood vessels. (E) Frontal section of E10.5 *Tie2-Cre; R26R* embryos showed strong *Tie2-Cre* expression only in the endothelium of pharyngeal arches (arrowhead). (F) High-power magnification of left fourth pharyngeal arch artery showed

endothelial expression of *Tie2-Cre* (arrowhead). H: Heart; III, IV and VI represent third, fourth and sixth pharyngeal arch arteries, respectively.

**Fig. 3** Foxc2 expression in *Nkx2.5-Cre* and *Tie2-Cre* mediated conditional knockouts in the pharyngeal arch arteries. Frontal sections of E10.5 *Foxc2* $^{fl/fl}$ (A), *Nkx2.5-Cre; Foxc2*$^{fl/fl}$ (D) and *Tie2-Cre; Foxc2*$^{fl/fl}$ (G) embryos were immunostained with an anti-Foxc2 antibody (green). Sections were co-stained with DAPI nuclear marker. (B-C, E-F, H-I) High-power images of the areas indicated by white boxes in panels A, D, G. (B-C) Foxc2 is strongly expressed in the mesenchymal cells (white arrow) and endothelium (arrowhead) of the left fourth pharyngeal artery. (E-F) Foxc2 is efficiently deleted in the derivatives of *Nkx2.5* expressing progenitors, i.e. in the mesenchyme (red arrow) and endothelium (red arrowhead) of the left fourth pharyngeal artery. (H-I) Foxc2 expression is reduced in the endothelium (red arrowhead) but unaffected in the mesenchymal cells (white arrow) in the left fourth pharyngeal arch artery of *Tie2-Cre; Foxc2*$^{fl/fl}$ mutant embryos.

**Fig. 4** Aortic arch abnormalities in *Foxc2* conditional knockout embryos at E18.5. (A) Gross dissections of control embryos show normal aortic arch formation. (B) *Nkx2.5-Cre; Foxc2*$^{fl/fl}$ conditional knockout embryos show aortic arch interruption type B, where part of LCCA and LSA is absent (arrow). (C) Normal aortic arch was formed in *Tie2-Cre; Foxc2*$^{fl/fl}$ conditional knockout embryos. (D-F) Schematic representation of the normal aortic arch (D, F) and type B aortic arch interruption (E). Pt, pulmonary trunk; Ao, aorta; aAo, arch of the aorta; BC, brachiocephalic artery; RSA, right subclavian artery; RCCA, right common carotid artery; LCCA; left common carotid artery; LSA, left subclavian artery; IAA-B; interrupted aortic arch type B.

**Fig. 5** *Nkx2.5-Cre* and *Tie2-Cre*-specific deletion of *Foxc2* showed ventricular septal defects and oedema. (A-C) Transverse sections of E18.5 heart of control and mutant embryos. Compared to control embryos (A), the loss of Foxc2 in *Nkx2.5-Cre* expressing precursors result in ventricular septum defect (VSD) (B, black arrow). In control and *Tie2-Cre; Foxc2*$^{fl/fl}$ embryos, we did not find any VSD. Ventricular septum is well separated from the left and right-sided pumping chambers (arrowhead, A&C). (D-F) Lateral views of control and conditional mutant embryos at E14.5. Control and *Nkx2.5-Cre; Foxc2*$^{fl/fl}$ embryos are normal in development (D-E). In *Tie2-Cre; Foxc2*$^{fl/fl}$ embryos, peripheral oedema was formed where fluid in the lymphatic system has accumulated (white arrow, F).

**Fig. 6** Abnormal aortic arch remodeling in *Nkx2.5-Cre; Foxc2*$^{fl/fll}$ embryos. Intracardiac ink injection was performed on E12.5 (A, B) and E13.5 (C, D) in control and mutant embryos. (A, B) At E12.5, no apparent aortic arch remodelling defect was found in control (A) or *Nkx2.5-Cre; Foxc2*$^{fl/fll}$ mutant embryos (B). (C, D) At E13.5, an aortic arch remodelling defect became apparent in mutant embryos (D) compared to control embryos (C). The red arrow in Fig C indicates the normal aortic arch formation and the red arrow in Fig D indicates interrupted aortic arch type B.

Fig 1

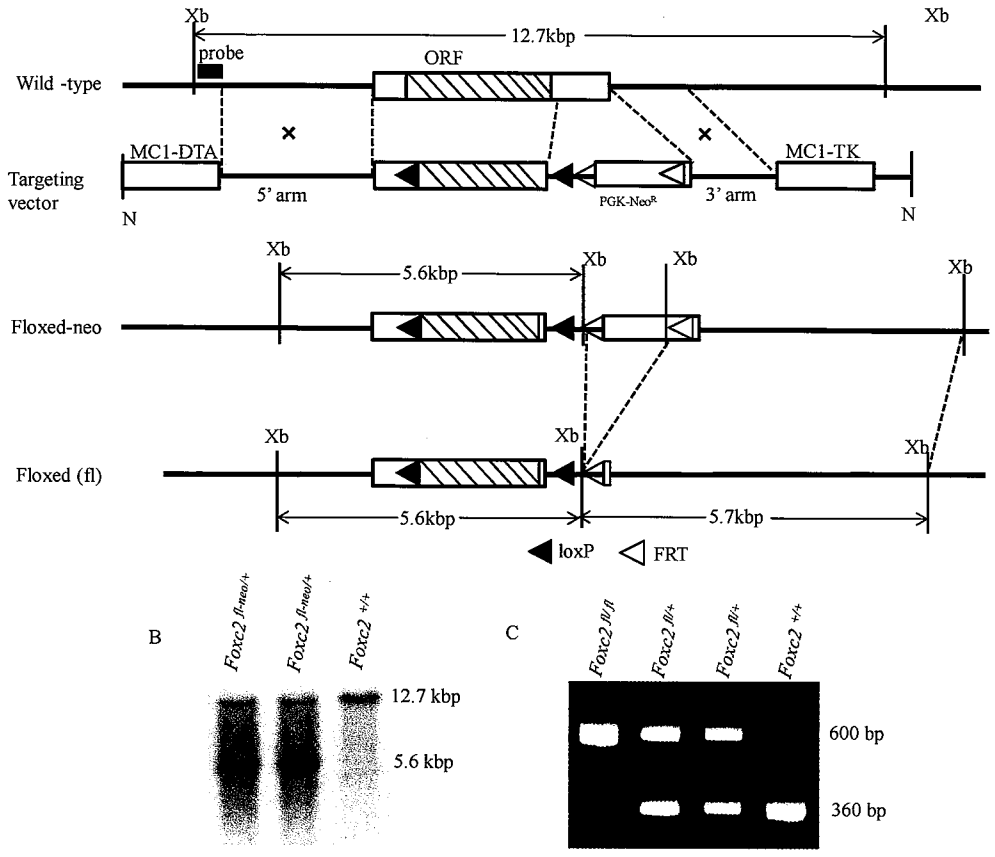
Xb
12.7kbp
Xb
probe
ORF
Wild -type
MC1-DTA
MC1-TK
Targeting vector
5' arm
PGK-Neo^R
3' arm
N
N
Xb
5.6kbp
Xb
Xb
Xb
Floxed-neo
Xb
Xb
Xb
Floxed (fl)
5.6kbp
5.7kbp
loxP
FRT
B
Foxc2 fl-neo/+
Foxc2 fl-neo/+
Foxc2 +/+
12.7 kbp
5.6 kbp
C
Foxc2 fl/fl
Foxc2 fl/+
Foxc2 fl/+
Foxc2 +/+
600 bp
360 bp

Fig 2

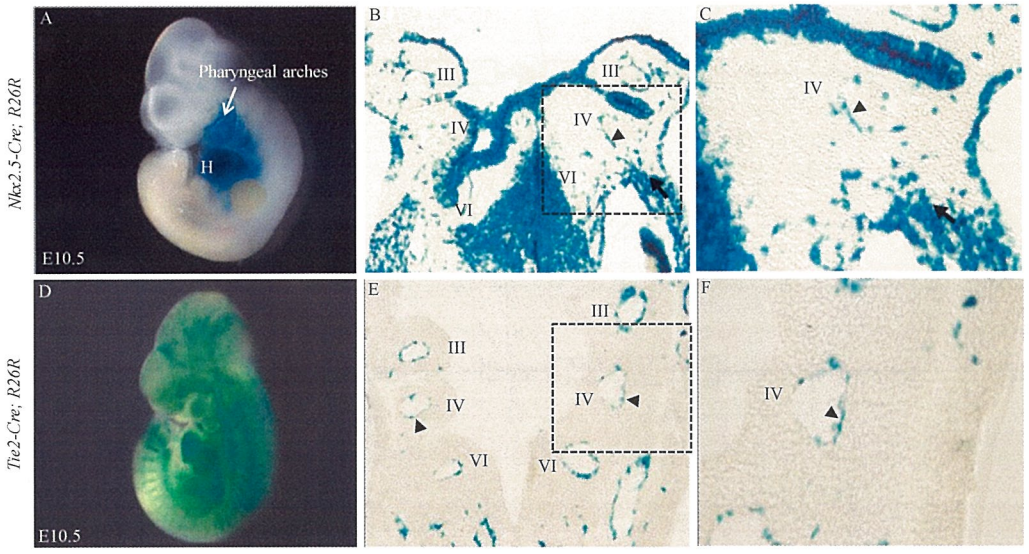
A
Pharyngeal arches
H
E10.5
B
III
III
IV
IV
VI
VI
C
IV
Nkx2.5-Cre; R26R
D
E10.5
E
III
III
IV
IV
VI
VI
F
IV
Tie2-Cre; R26R

Fig 3

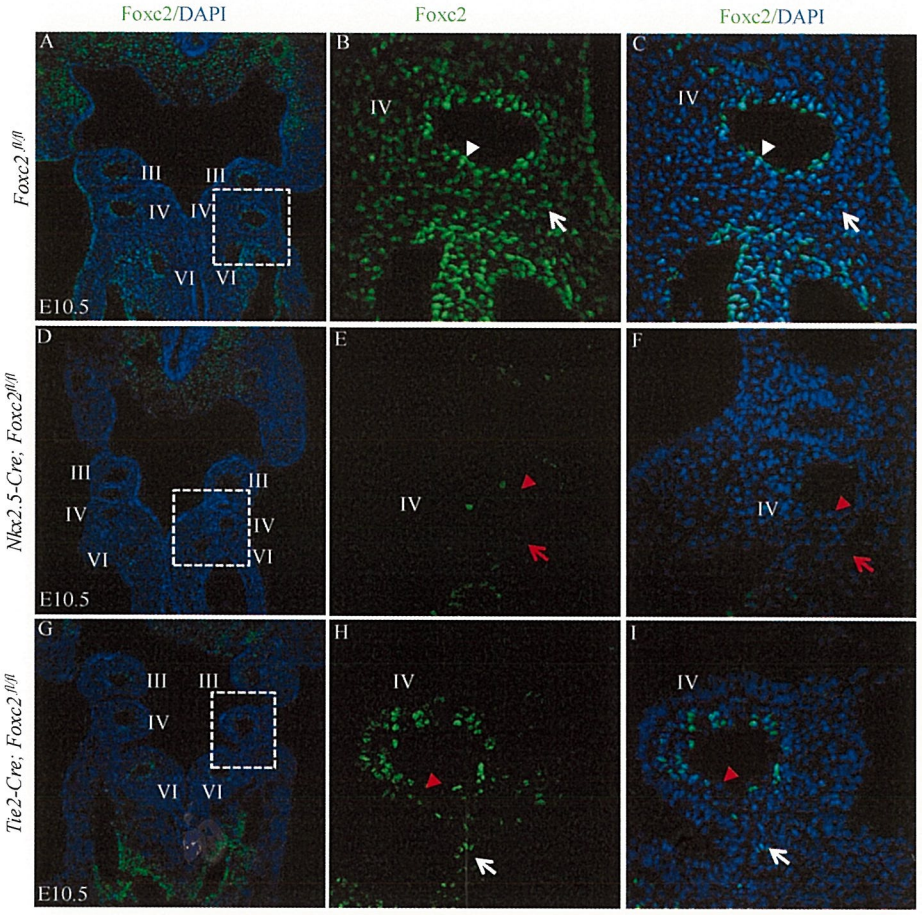
Foxc2/DAPI
Foxc2
Foxc2/DAPI
A
B
C
D
E
F
G
H
I
III
IV
VI
E10.5
Foxc2 fl/fl
Nkx2.5-Cre; Foxc2 fl/fl
Tie2-Cre; Foxc2 fl/fl

Fig 4

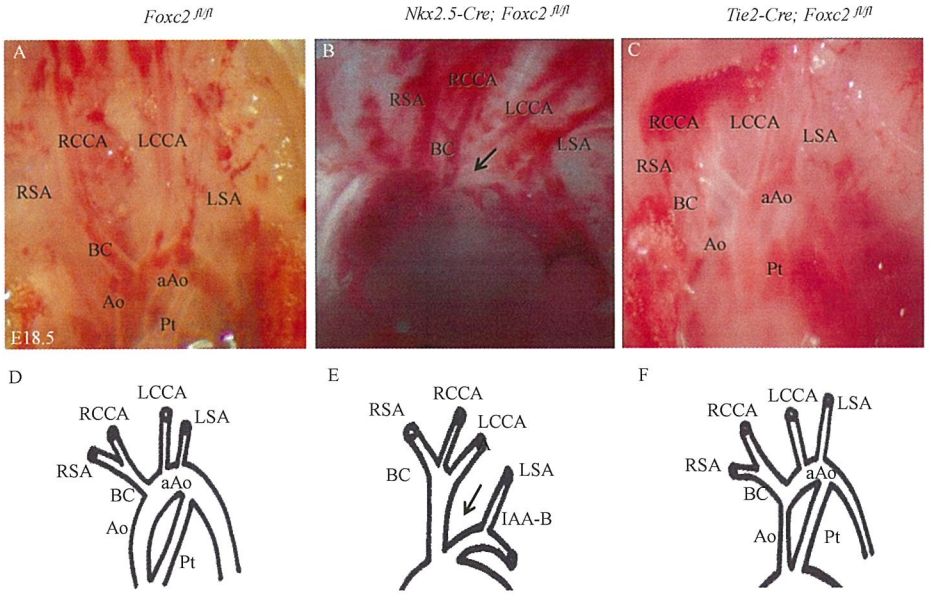
Foxc2 fl/fl
Nkx2.5-Cre; Foxc2 fl/fl
Tie2-Cre; Foxc2 fl/fl
A
RCCA
LCCA
RSA
LSA
BC
aAo
Ao
Pt
E18.5
B
RCCA
RSA
LCCA
BC
LSA
C
RCCA
LCCA
LSA
RSA
BC
aAo
Ao
Pt
D
LCCA
RCCA
LSA
RSA
BC
aAo
Ao
Pt
E
RCCA
RSA
LCCA
BC
LSA
IAA-B
F
LCCA
RCCA
LSA
RSA
aAo
BC
Ao
Pt

Fig 5

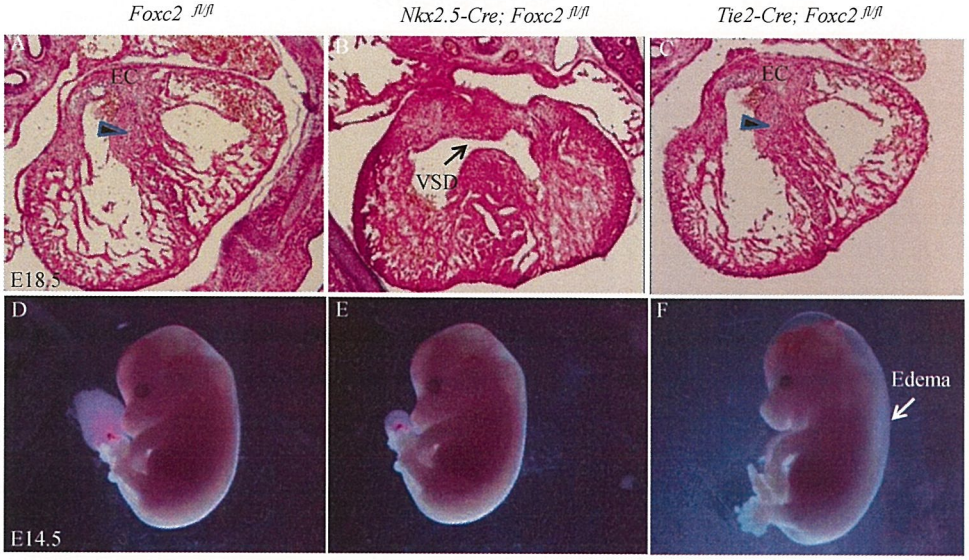
Foxc2 fl/fl
Nkx2.5-Cre; Foxc2 fl/fl
Tie2-Cre; Foxc2 fl/fl
A
EC
E18.5
B
VSD
C
EC
D
E14.5
E
F
Edema

Fig 6